Anisotropic 2D Diffusive Expansion of Ultracold Atoms in a Disordered Potential

M. Robert-de-Saint-Vincent, J.-P. Brantut,[†] B. Allard, T. Plisson, L. Pezzé, L. Sanchez-Palencia, A. Aspect, T. Bourdel,[*] and P. Bouyer

Laboratoire Charles Fabry de l'Institut d'Optique, Univ. Paris Sud, CNRS, campus polytechnique RD128, 91127 Palaiseau France

(Received 2 April 2010; published 2 June 2010)

We study the horizontal expansion of vertically confined ultracold atoms in the presence of disorder. Vertical confinement allows us to realize a situation with a few coupled harmonic oscillator quantum states. The disordered potential is created by an optical speckle at an angle of 30° with respect to the horizontal plane, resulting in an effective anisotropy of the correlation lengths of a factor of 2 in that plane. We observe diffusion leading to non-Gaussian density profiles. Diffusion coefficients, extracted from the experimental results, show anisotropy and strong energy dependence, in agreement with numerical calculations.

DOI: 10.1103/PhysRevLett.104.220602 PACS numbers: 05.60.Gg, 37.10.Gh, 67.85.Hj, 73.50.Bk

Transport in most materials is determined by the complex interplay of many ingredients, for instance the structure and thermal fluctuations of the substrate [1], the interparticle interactions, which can induce superconductivity [2] or metal-insulator transitions [3], and disorder [4]. Disorder is relevant to many condensed-matter systems and strongly affects transport via scattering. Its primary effect is thus diffusion, an effect underlying the Drude theory of conductivity [1], as well as the self-consistent theory of Anderson localization [5]. Disorder is of special interest in dimension two (2D), which is the marginal dimension for return probability in Brownian motion and for Anderson localization [6]. Moreover, intriguing effects, which are not fully understood, occur in 2D, such as the metal-insulator transitions in high-mobility Si MOSFETs [7,8], GaAs heterostructures [9,10], and thin metal-alloy films [11].

Ultracold atomic gases are good candidates to study classical or quantum disordered systems (see Refs. [12,13], and references therein). They offer unique versatility as one can control the amount and type of disorder, the interaction strength or the confinement geometry. In 1D, Anderson localization [14,15] and interaction-induced delocalization [16] have been observed. In 3D, the competition between interaction and disorder has been investigated in disordered optical lattices [17,18]. Diffusion was reported for speckle-induced 3D optical molasses in the dissipative regime [19]. So far, less work has been devoted to 2D.

In this Letter, we study diffusion of ultracold atoms in an effectively anisotropic disordered potential without dissipation. The geometry is planar as the atoms are confined vertically to a size of about 1 μm in a dipole trap and horizontally free to move over a millimeter. In the presence of disorder, we observe expansion at a reduced speed and anisotropic, non-Gaussian atomic density profiles. We show that the dynamics is horizontally diffusive. Fitting a diffusive model to the data, we extract the diffusion coefficients and find that they are anisotropic and strongly energy-dependent. Our results are consistent with numerical simulations assuming classical dynamics.

The experimental setup uses a vertically confining potential and a speckle light field (see Fig. 1). Both are created with 767 nm laser light [20], blue detuned from the resonance at 780 nm for ^{87}Rb atoms in their ground state. They thus induce a repulsive potential. The vertical confinement is realized between the two lobes of a vertically focused Hermite-Gauss TEM01-like mode, prepared with a holographic $0-\pi$ phase plate [21,22]. The measured vertical trapping frequency is $\omega/2\pi = 680$ Hz with a 22 μm separation between the two intensity maxima, a total power of 150 mW, and an horizontal waist radius at $1/e^2$ of 1.1 mm.

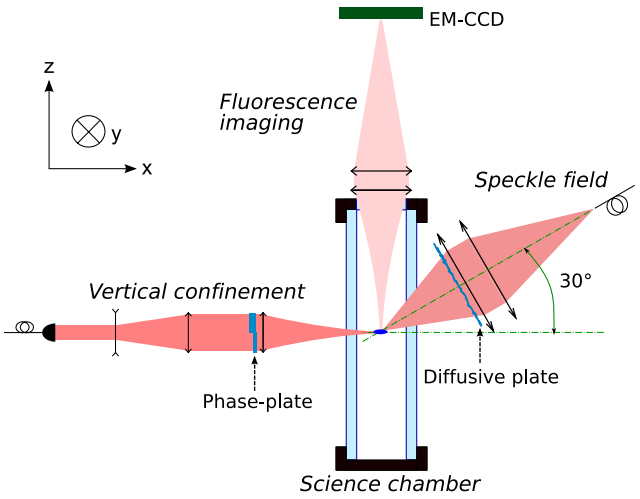

FIG. 1 (color online). Experimental setup (see details in text). Atoms are detected from the top by fluorescence imaging on an Andor electron multiplying charge coupled device (EM-CCD).

The speckle light field is produced by a beam passing through a diffusive plate [23,24] and focused on the atoms. The high numerical aperture (a 75 mm diameter aperture at a distance of 150 mm from the atoms) allows us to achieve an approximately Gaussian correlation function with transverse correlation length $\sigma_y = 0.8\ \mu$m (half-width at $1/\sqrt{e}$). The longitudinal correlation length (in the direction of propagation) is deduced to be $\sigma_{\text{long}} \approx 9\ \mu$m [24]. As the speckle beam is at 30° from the horizontal expansion plane, the correlation length σ_x along x is $2\sigma_y = 1.6\ \mu$m. With a power of 66 mW and a Gaussian waist radius of 1.1 mm, at the center of the beam, the standard deviation of the disordered repulsive potential (equal to its average value) is $\bar{V} \approx k_B \times 53(8)$ nK $\approx (2\pi\hbar) \times 1.1(2)$ kHz (where k_B is the Boltzmann constant and $2\pi\hbar$ the Planck constant).

The experiment proceeds as follows. An ultracold atom sample is produced by an all-optical runaway evaporation in a crossed dipole trap at 1565 nm, as described in Ref. [25]. The atom cloud is first transferred in 5 ms in a trap combining simultaneously the initial crossed dipole trap and the vertically confining beam. The crossed trap is then further ramped down in 200 ms in order to reduce the confinement and thus also the temperature to $k_B T \approx k_B \times 200(20)$ nK $\approx (2\pi\hbar) \times 4.2(4)$ kHz, slightly above the condensation threshold. Finally, the speckle field is ramped up in 4 ms, and 1 ms later a thermal cloud of $N = 1.5 \times 10^5$ atoms is released in the horizontal plane by suddenly turning off the crossed dipole trap. After a chosen 2D expansion time, the vertical confinement and the speckle potential are switched off. After 0.1 ms, the atomic column density is measured from the top through fluorescence imaging.

A typical image for an expansion time of 50 ms in the disordered potential is presented in Fig. 2(a). The corresponding integrated density along y (respectively x) is plotted in Fig. 2(b) [respectively 2(c)]. We observe a sharp anisotropic structure elongated along x around the initial position, surrounded by a broader isotropic cloud similar to what is observed in the absence of disorder. The sharp anisotropic structure corresponds to low energy atoms, whose expansion has been slowed down by the disorder, whereas the broad cloud corresponds to atoms which expand almost ballistically at this time scale. For an expansion time of 200 ms [see Figs. 2(b) and 2(c)], the contribution of the ballistic atoms is negligible with respect to the lowest energy atoms. The cloud profiles are then found to be non-Gaussian with long tails in both directions. Similar profiles have been theoretically predicted for energy-dependent diffusive behavior in the expansion of Bose-Einstein condensates [26].

We first study the behavior of the peak column density $n(0, 0, t)$ as a function of time. It should scale as $1/t$ in a diffusive regime, and as $1/t^2$ for a ballistic expansion. Figure 3 shows a log-log plot of the measured peak density as a function of time. For times below 15 ms, the cloud is smaller than the pixel size and therefore our measurement does not reflect $n(0, 0, t)$. Between 15 and 200 ms, we observe a linear behavior with a slope $-2.0^{-0.2}_{+0.3}$ without disorder, whereas with disorder, we find a linear behavior with a slope $-1.0^{-0.1}_{+0.3}$. The uncertainties come from the dispersion of the slopes found for different data sets taken in similar conditions. This measurement is consistent with diffusive expansion of a significant part of the atoms in the horizontal plane. After only 15 ms, the contribution of the

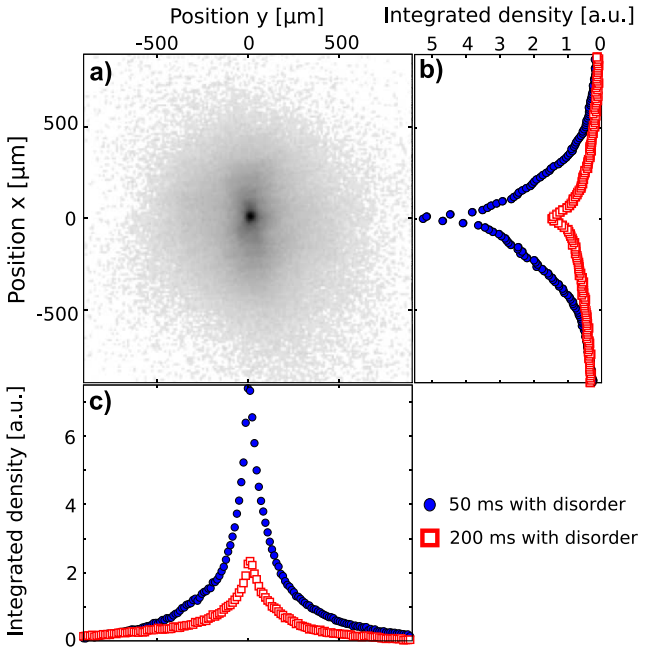

FIG. 2 (color online). Atomic column density after planar expansion of an ultracold gas in an anisotropic speckle potential. (a) Image after 50 ms of expansion. (b),(c) Integrated density along the two major axes. The plain dots (open squares) correspond to 50 ms (200 ms) of expansion.

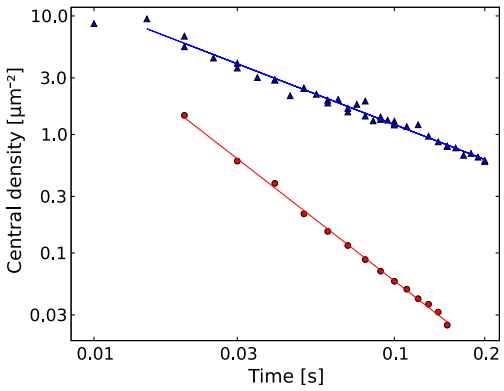

FIG. 3 (color online). Evolution of the peak column density $n(0, 0, t)$ as a function of expansion time. Triangles: with disorder; circles: without disorder. The solid lines are fits with algebraic time dependence between 15 and 200 ms. The fitted slopes of the decay are -0.98 with disorder and -1.97 without disorder.

ballistically expanding atoms to the density at the origin vanishes.

In order to understand our experimental findings in more detail, we have performed numerical simulations. In the experiment, $k_B T \approx 6\hbar\omega$, so that a few vertical harmonic oscillator states are populated. The vertical size of the atomic cloud, $\Delta z \simeq \sqrt{k_B T/m\omega} \approx 1\ \mu$m (where m is the atom mass), is much smaller than σ_{long} and the speckle potential can be considered invariant along its propagation axis. Since it makes an angle $\theta = 30°$ with respect to the expansion plane, it couples the vertical quantum states. To account for these features in the numerics, we consider the 3D dynamics of classical particles in the external potential $V(x, y, z) + m\omega^2 z^2/2$, with $V(x, y, z) = V_{\text{iso}}(x\sin\theta - z\cos\theta, y)$ where $V_{\text{iso}}(u, v)$ is a 2D *isotropic* speckle potential with correlation length σ_y. Using a classical particle model is a reasonable approximation since $k_B T/\hbar\omega \approx 6$ and $k\sigma_y \approx 5$ where $k = \sqrt{mk_B T}/\hbar$. Note also that our experiment is not in the weak scattering limit [27] as $(\bar{V}/k_B T)^2 (k\sigma_y)^2 \approx 1.6$.

A characteristic time scale for the dynamics is the Boltzmann time τ_B, i.e., the time after which the memory of the direction is lost, which depends on the particle energy. For long times ($t \gg \tau_B$), scattering from the angled speckle potential redistributes the kinetic and potential energies in 3D, so that the dynamics in the horizontal plane is expected to depend on the 3D particle energy E. We hence calculate the spatial variances $\langle \xi^2(E, t)\rangle$ as a function of time, where $\xi = x, y$ and brackets indicate averaging over disorder and over initial conditions corresponding to the energy E. The evolution is described by $\langle \xi^2(E, t)\rangle \simeq 2D_\xi(E) t^{\gamma_\xi(E)}$. We identify three regimes characterized by the value of $\gamma_\xi(E)$. For $E/\bar{V} \lesssim 2$, we find a subdiffusive dynamics, i.e., $\gamma_\xi(E) < 1$, for experimentally relevant time scales. In particular, for $E/\bar{V} \lesssim 0.52$, we find strictly bounded trajectories, $\gamma_\xi(E) = 0$. This is consistent with the percolation threshold expected for 2D speckle potentials [28,29]. For $E/\bar{V} \gtrsim 2$, numerical simulations yield a diffusive dynamics, i.e., $\gamma_\xi(E) \simeq 1$. In this regime, the diffusion coefficients $D_\xi(E)$ are strongly anisotropic and grow algebraically with the particle energy [Fig. 4(a)]. From a fit to the numerical calculations for our parameters, we find $D_x(E) = 2.4\sqrt{\bar{V}\sigma_y^2/m}(E/\bar{V})^{2.8}$ and $D_y(E) = 0.65\sqrt{\bar{V}\sigma_y^2/m}(E/\bar{V})^{2.8}$ [30,31]. We have also done simulations of a classical 2D diffusion in the same anisotropic disorder. The various regimes found in the 3D simulations with vertical confinement are also found in 2D simulations at the same values of $E/\bar{V}$. In the diffusive regime, the energy dependence of the diffusion coefficients remains algebraic but with modified constants.

In the experiment, the observed expansion results from the diffusion of atoms with a broad energy distribution, $N(E)$. It can be calculated assuming that, before abrupt release in the horizontal plane, the gas is at thermal equilibrium in the trap plus speckle potential. The corresponding energy distribution $N(E) \propto e^{-E/k_B T} \sum_{n=0}^{E/\hbar\omega} (1 - e^{(n\hbar\omega - E)/\bar{V}})$ is plotted in Fig. 4(b) [32]. It is fully determined from the experimental parameters ω, N, $\bar{V}$, and T. Here, only 6% of the atoms are subdiffusive [$E \leq 2\bar{V}$, shaded regions in Fig. 4(b)]. Incorporating their contribution to the diffusive regime is thus a small error, and for long expansion time, the column density can be approximated by

$$n(x, y, t) \simeq \int_0^\infty dE N(E) \frac{1}{t} \frac{\exp(-\frac{x^2}{4D_x(E)t} - \frac{y^2}{4D_y(E)t})}{4\pi\sqrt{D_x(E)D_y(E)}}. \quad (1)$$

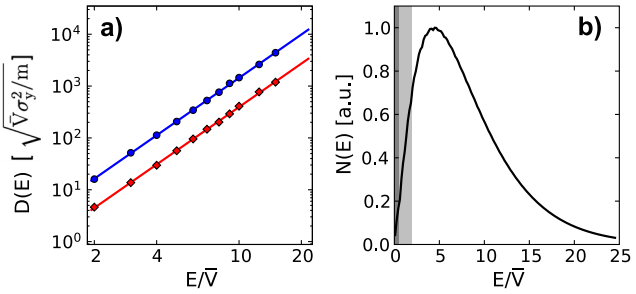

FIG. 4 (color online). (a) Diffusion coefficients along x (blue circles) and y (red diamonds) as a function of energy in log-log scale. Points are numerical results, lines are fits to power laws. (b) Energy distribution for the experimental parameters. The shaded regions correspond to subdiffusive regimes (see text).

We fit Eq. (1) (convolved with our imaging resolution $\sim 15\ \mu$m) to the experimental 2D density distribution with $D_x(E) = D_x^0(E/E_R)^\alpha$ and $D_y(E) = D_y^0(E/E_R)^\alpha$, D_x^0, D_y^0, and α as fitting parameters, and the recoil energy $E_R = k_B \times 180$ nK as energy scale. As can be seen on Fig. 5, the 2D fit function reproduces the data both close to the central peak and in the wings. We find $D_x^0 = 3.0(1.5) \times 10^{-7}\ \text{m}^2\,\text{s}^{-1}$, $D_y^0 = 8.7(4.3) \times 10^{-8}\ \text{m}^2\,\text{ms}^{-1}$, and $\alpha = 3.3(3)$. The uncertainties come from the uncertainties on the measurements of N, $\bar{V}$, and T used in $N(E)$ and from an observed systematic drift of the results as a function of the expansion time [33]. Experimentally, the power-law exponent is found to be $\alpha = 3.3(3)$, to be compared with 2.8 in the simulation. The observed ratio of the two diffusion coefficients is 3.45(15) when it is 3.7 in the simulation. These slight discrepancies can be due to the approximations made in order to derive Eq. (1). At $E = E_R \approx k_B T$, numerically, we find $D_x(E_R) = 1.3(0.6) \times 10^{-7}\ \text{m}^2\,\text{s}^{-1}$ and $D_y(E_R) = 3.5(1.7) \times 10^{-8}\ \text{m}^2\,\text{s}^{-1}$, where the uncertainties come from the uncertainties on $\bar{V}$ and σ_y. The experimental values of the diffusion coefficients are thus in quantitative agreement with the 3D classical simulation.

In conclusion, we have observed and studied 2D diffusive expansion of ultracold atoms in a disordered potential. As a result of the effective anisotropy of the speckle potential, the diffusion is anisotropic. Fitting a diffusive model to our density profiles, we are able to extract the

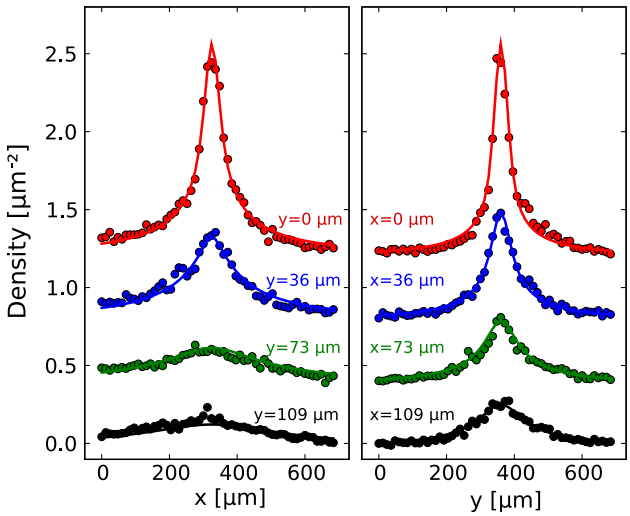

FIG. 5 (color online). 2D density distribution after 200 ms of expansion. Density profiles through cuts along x (respectively y) at different positions along y (respectively x). The upper (red) points are cuts through the central peak, whereas the other curves downward correspond to positions separated by ~ 36 μm. They are artificially offset for clarity. The lines are the result from the 2D fit with Eq. (1) convolved by the imaging resolution (~ 15 μm).

diffusion coefficients and find a strong dependence on the atom energy, in quantitative agreement with a classical simulation for our parameters.

Understanding the diffusion properties as a function of energy (in particular out of the weak scattering regime) is a necessary step towards the study of other disorder-induced effects in two dimensions, starting with anomalous subdiffusion [34] and classical trapping under the percolation threshold [28,29]. By cooling the gas further or by reducing the correlation length of the disorder, we expect quantum corrections to the diffusion and Anderson localization to show up at the sub-mm length scale of the experiment [27]. Moreover, in a 2D degenerate gas, the influence of disorder on the Berezinskii-Kosterlitz-Thouless transition [35] is especially intriguing. Will the vortices be pinned by disorder [36]?

We thank F. Moron and A. Villing for technical assistance, M. Besbes and GMPCS high performance computing facilities of the LUMAT federation for numerical support. This research was supported by CNRS, CNES as part of the ICE project, Direction Générale de l'Armement, ANR-08-blan-0016-01, IXSEA, EuroQuasar program of the EU. LCFIO is member of IFRAF.

*Corresponding author.
thomas.bourdel@institutoptique.fr
†Present address: ETH Zürich, 8093 Zürich, Switzerland.

[1] N. W. Ashcroft and N. D. Mermin, *Solid State Physics* (Saunders, Philadelphia, USA, 1976).
[2] P.-G. de Gennes, *Superconductivity of Metals and Alloys* (Benjamin, New York, 1966).
[3] N. Mott, Rev. Mod. Phys. **40**, 677 (1968).
[4] P. Anderson, Phys. Rev. **109**, 1492 (1958).
[5] D. Vollhardt and P. Wölfle, Phys. Rev. Lett. **45**, 842 (1980).
[6] E. Abrahams, P. W. Anderson, D. C. Licciardello, and T. V. Ramakrishnan, Phys. Rev. Lett. **42**, 673 (1979).
[7] E. Abrahams, S. V. Kravchenko, and M. P. Sarachik, Rev. Mod. Phys. **73**, 251 (2001).
[8] S. V. Kravchenko and M. P. Sarachik, Rep. Prog. Phys. **67**, 1 (2004).
[9] G. Allison *et al.*, Phys. Rev. Lett. **96**, 216407 (2006).
[10] L. A. Tracy *et al.*, Phys. Rev. B **79**, 235307 (2009).
[11] Y. Dubi, Y. Meir, and Y. Avishai, Nature (London) **449**, 876 (2007).
[12] L. Fallani, C. Fort, and M. Inguscio, *Advances in Atomic, Molecular, and Optical Physics* (Academic Press, New York, 2008), Vol. 56, p. 119.
[13] L. Sanchez-Palencia and M. Lewenstein, Nature Phys. **6**, 87 (2010).
[14] J. Billy *et al.*, Nature (London) **453**, 891 (2008).
[15] G. Roati *et al.*, Nature (London) **453**, 895 (2008).
[16] B. Deissler *et al.*, Nature Phys. **6**, 354 (2010).
[17] M. White *et al.*, Phys. Rev. Lett. **102**, 055301 (2009).
[18] M. Pasienski, D. McKay, M. White, and B. DeMarco, arXiv:0908.1182.
[19] G. Grynberg, P. Horak, and C. Mennerat-Robilliard, Europhys. Lett. **49**, 424 (2000).
[20] G. Stern *et al.*, arXiv:1003.4761.
[21] T. P. Meyrath, F. Schreck, J. L. Hanssen, C.-S. Chuu, and M. G. Raizen, Opt. Express **13**, 2843 (2005).
[22] N. L. Smith, W. H. Heathcote, G. Hechenblaikner, E. Nugent, and C. J. Foot, J. Phys. B **38**, 223 (2005).
[23] J. W. Goodman, *Speckle Phenomena in Optics* (Roberts, Greenwood Village, Colorado, 2007).
[24] D. Clément *et al.*, New J. Phys. **8**, 165 (2006).
[25] J.-F. Clément *et al.*, Phys. Rev. A **79**, 061406(R) (2009).
[26] B. Shapiro, Phys. Rev. Lett. **99**, 060602 (2007); L. Beilin, E. Gurevich, and B. Shapiro, Phys. Rev. A **81**, 033612 (2010).
[27] R. C. Kuhn, O. Sigwarth, C. Miniatura, D. Delande, and C. A. Müller, New J. Phys. **9**, 161 (2007).
[28] L. N. Smith and C. J. Lobb, Phys. Rev. B **20**, 3653 (1979).
[29] A. Weinrib, Phys. Rev. B **26**, 1352 (1982).
[30] An algebraic increase of the diffusion coefficients with the energy is also found in the weak scattering limit for isotropic speckle potentials, with $\gamma = 2.5$ [27].
[31] The numerical factors depend on $\hbar\omega/\bar{V}$ and σ_x/σ_y.
[32] The vertical harmonic oscillator is quantized and the zero point energy is taken as the energy of the ground state.
[33] For atoms with energy $k_B T$, we find $\tau_B \sim 50$ ms and these atoms behave almost diffusively after 200 ms. However, some atoms with larger energy remain ballistic over the time scale of the experiment. These atoms could be responsible for the observed drift.
[34] R. Metzler and J. Klafter, Phys. Rep. **339**, 1 (2000).
[35] Z. Hadzibabic, P. Krüger, M. Cheneau, B. Battelier, and J. Dalibard, Nature (London) **441**, 1118 (2006).
[36] S. Tung, V. Schweikhard, and E. A. Cornell, Phys. Rev. Lett. **97**, 240402 (2006).